Journal of Innovative Optical Health Sciences
Vol. 2, No. 2 (2009) 137–142

World Scientific
www.worldscientific.com

RESEARCH ON THE MOIRE CHROMATOGRAPHY TECHNIQUE AND ITS APPLICATION

TIANZE LI* and SHUYUN WANG
School of Electrical and Electronic Engineering
Shandong University of Technology
Zibo 255049, China
**ltzwang@163.com*

This paper explains the Moire chromatography technique and the optical characteristics when the light crosses the 3D air flow field. Based on this, taking grating, CCD camera, optical filter and diaphragm as the main device, a multi-direction Moire chromatography optical system was designed. The system consists of five detective light paths, in each detective light path there is parallel and same periodic grating and filtering minipore placed on the lens' focal length plane; the grating is used to adjust the space length and angle between the two gratings, and the filtering minipore is used to remove the unorderly high frequency intermix in the Moire fringe. Utilizing the computer escalator method to convert the tested value, the vivid interference fringe of tested parameter can be obtained. The application of this system in precision measurement and medicine is also analyzed and discussed.

Keywords: Moire chromatography optical system; computer escalator method; medicine.

1. Introduction

There has been plenty literature and news on utilizing the optics-interference method to study the compressible air density field and plasma diagnosis in three-dimensional (3D) air flow, wind tunnel and shock tube. However, the researches on these fields are only limited to the symmetrical 2D or 3D distribution so far, involving only one directional interference pattern. There is quantitative analysis about the temperature and density field of 2D and axial symmetrical distribution, however, it is difficult to realize the symmetry in practice. For temperature and density field dissymmetrical distribution, multi-directional interference patterns are needed to realize the 3D temperature and density field. So the key problem is how to build the Moire deflection system and computer tomography arithmetic in order to realize the back analysis on temperature and density field.[1,2]

In this paper, the optics interference and Moire chromatography technique theory are expounded firstly, and based on that a multi-directional Moire chromatography system is designed, and then the parameters (temperature and pressure etc) of 3D air-flow field are tested using the computer tomography arithmetic and Moire chromatography technique. The system will have wide application in medical projects.

2. Basic Principle of Moire Chromatography Technique

2.1. *Beam deflect effect*

Fermat principle points out that when light waves spread in dissymmetrical medium, its wave surface (equiphase surface) will turn into aberrance. In symmetrical medium, the light follows a beeline; in dissymmetrical medium, the light follows a curve, i.e., while the light passes through the dissymmetrical refractive index field, the deflect effect of light is produced. It is shown in Fig. 1.

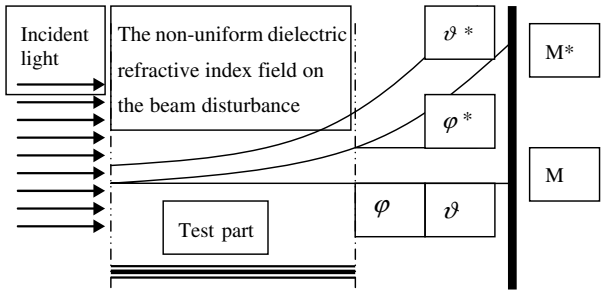

Fig. 1. Deflection of light beam in non-uniform medium refractive index field.

2.2. *Formation and characteristic of Moire pattern*

The two grating surfaces are made congruent, in order to make the bar-line to form the wee angle. When light shines through the crack, the bright and dark Moire pattern will be produced, as shown in Fig. 2. The relation and main characteristic among space, bar pitch and angle of Moire pattern are that: (1) average effect — because Moire pattern is produced by plenty of reticles of gratings, it has some average function to the scale error of grating; (2) magnification function — when the two gratings move a bar-pitch comparatively, Moire pattern moves also; (3) corresponding relation — there is relation between the mobile volume, mobile direction of Moire pattern and displacement volume, displacement direction of grating scale.

Utilizing the functions, the angle of light through the temperature field and density field can be obtained accurately, then the temperature and density of air can be obtained by means of refraction angle. If the tested parameters of high-temperature air-flow field, density etc are dissymmetric or asymmetric, the data of Moire pattern can be measured from different directions and different angles, at the same time we can back-analyze distribution of the temperature field and density field by using the computer tomography technique.[3,4]

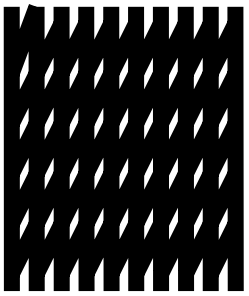

Fig. 2. Moire pattern.

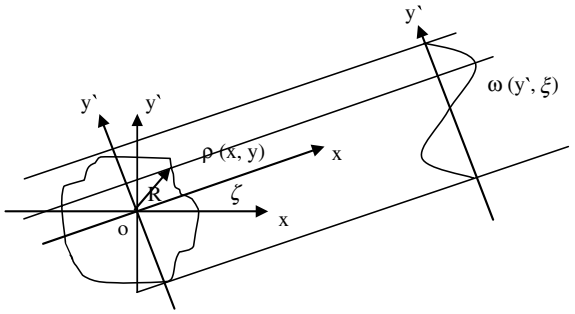

Fig. 3. Fixed and turning coordinate systems for the test field.

2.3. *Deflection analysis of Moire pattern on the transformation coordinate*

In Fig. 3, it shows that there is an angle ξ between the two gratings on the two coordinates. On the x-y coordinate, the density distribution of temperature field is $\rho(x, y)$, and on y'-ξ coordinate, the deflection distribution of Moire pattern is $\omega(y', \xi)$. The data of Moire pattern are tested by means of parallel beams shining around the experiment area. The deflection pattern is in direct proportion to the whole density grads of the normal observation light path direction. The relation between density $\rho(x, y)$ and Moire deflection $\omega(y', \xi)$ is:

$$\omega(y', \xi) = \int_{-R}^{R} \frac{\partial f(x, y)}{\partial y'} dx'. \tag{1}$$

$f(x, y)$ is the refractive index:

$$f(x, y) = \frac{\beta\Delta[\rho(x, y) - \rho_s]}{\theta\rho_n}, \tag{2}$$

where β is degree on which the air refractive index depends on the intensity; Δ is the distance of the two adjacent grid lines; θ is the angle of the two grid lines; ρ_s is the density of tested temperature field; ρ_n is the density of temperature field under standard circumstance; and R is the curvature radius of tested area.

3. Computer Simulation Algorithm

If higher precision is needed, the proper algorithm is required. We rebuild the refractive index in formula (1). The rebuilding temperature field is divided into $L = M * N$ pixels, so the space is d_x, d_y. Expand the $f(x, y)$ into series:

$$f(x, y) = \sum_i \sum_j f_{ij} b_{ij}(x, y). \tag{3}$$

The deflection angle of line beam is

$$\omega(y',\xi) = \sum_i \sum_j f_{ij} \int \frac{\partial b_{ij}}{\partial y'} dx'. \tag{4}$$

Suppose $G_{ij}(y',\xi) = \int \frac{\partial b_{ij}}{\partial y'} dx'$, then

$$\omega(y',\xi) = \sum_i \sum_j f_{ij} G_{ij}(y',\xi). \tag{5}$$

3.1. *Series* $\sin c$ *expansion method*

Supposed that b_{ij} expands according to series $\sin c$:

$$b_{ij}(x,y) = \sin c\left[\frac{1}{d_x}(x - id_x)\right] \sin c\left[\frac{1}{d_y}(y - jd_y)\right]. \tag{6}$$

From the sample theorem,

$$\bar{f}(x,y) = \sum_{i=0}^{M-1} \sum_{j=0}^{N-1} \bar{f}(id_x, jd_y) \times \sin c\left[\frac{1}{d_x}(x - id_x)\right] \cdot \sin c\left[\frac{1}{d_x}(y - jd_y)\right], \tag{7}$$

where $\bar{f}(x,y)$ is the approximation of $\bar{f}(x,y)$. If we put formula (7) into line-beam difference base equation of single line beam, we can obtain:

$$\sum_{i=0}^{M-1} \sum_{j=0}^{N-1} \bar{f}(id_x, jd_y) \int \sin c\left[\frac{1}{d_x}(x - id_x)\right] \times \sin c\left[\frac{1}{d_y}(y - jd_y)\right] dx' = \psi(p_m, \xi_n) \tag{8}$$

and

$$\sum_{i=0}^{M-1} \sum_{j=0}^{N-1} \bar{f}(id_x, jd_y) \times \int_{-\infty}^{\infty} \sin c\left(\frac{x - id_x}{d_x}\right) \cdot \sin c\left(\frac{y - jd_y}{d_y}\right) \times (1 + a_n^2)^{1/2} dx = \psi(p_m, \xi_n). \tag{9}$$

From $x' = x - id_x$, $y' = y - jd_y$, then the line beam equation of parameter (p_m, ξ_n) is

$$y' = a_n x' + b'_{mn}. \tag{10}$$

Then the formula (9) will turn into

$$\sum_{i=0}^{M-1} \sum_{j=0}^{N-1} \bar{f}(id_x, jd_y) \times \int_{-\infty}^{+\infty} \sin c\left(\frac{x'}{d_x}\right) \cdot \sin c\left(\frac{a_n x' + b'_{mn}}{d_y}\right) \times (1 + a_n^2)^{1/2} dx' = \psi(p_m, \xi_n). \tag{11}$$

If $a_n \neq 0$, then

$$(1 + a_n^2)^{1/2} \sum_{i=0}^{M-1} \sum_{j=0}^{N-1} \bar{f}(id_x, jd_y) \int_{-\infty}^{+\infty} \sin c\left(\frac{x'}{d_x}\right) \cdot \sin c\left[\frac{a_m}{d_y}(q_{mn} - x')\right] dx' = \psi(p_m, \xi_n), \tag{12}$$

where $q_{mn} = -b'_{mn}/a_n$. Use the symmetry of $\sin c$, by means of 2D Fourier transform, formula (12) can be turned into:

$$\int_{-\infty}^{\infty} \sin c\left(\frac{x'}{d_x}\right) \sin c\left[\frac{a_n}{d_x}(q_{mn} - x')\right] dx' = F^{-1}\left[\frac{|d_x||d_y|}{|a_n|} rect\left(\frac{d_y f_y}{a_n}\right)\right], \tag{13}$$

where $rect(x) \equiv \begin{cases} 1, & |x| \leq 1/2 \\ 0, & |x| > 1/2 \end{cases}$ is the Fourier transform of $\sin c(x)$. Summing up the above, we can export:

$$b'_{mn} = p_m \sec(\xi_n) + id_x \tan(\xi_n) - jd_y. \tag{14}$$

The algebraic equation of $\bar{f}(id_x, jd_y)$ is

$$\sum_{i=0}^{M-1} \sum_{j=0}^{N-1} W_{ij}(p_m, \xi_n) \bar{f}(id_x, jd_y) = \Psi(p_m, \xi_n). \tag{15}$$

Thereinto

$$W_{ij}(p_m, \xi_n) = \begin{cases} (1 + \tan^2 \xi_n)^{1/2} d_x \sin c[p_m \sec \xi_n \\ \quad + id_x \tan \xi_n - jd_y)/d_y] \\ (0 \leq |\tan \xi_n| \leq d_y/d_x) \\ (1 + \tan^2 \xi_n)^{1/2} (d_y/|\tan \xi_n|) \sin c \\ \quad \cdot [p_m \sec \xi_n + id_x \tan \xi_n \\ - jd_y]/d_x \tan \xi_n] \\ (d_y/d_x < |\tan \xi_n| < \infty \\ \quad d_y \sin c[(p_m + id_x)/d_x] \\ (\tan \xi_n \to \pm\infty) \end{cases}. \tag{16}$$

3.2. *Computer network algorithm*

In Fig. 4, the refractive index $f(x,y)$ is a group of rectangular functions, the sample value $\bar{f}(id_x, jd_y)$'s weight is a rectangular function $rect[(x - id_x)/d_x] \cdot rect[(y - jd_y)/d_y]$, then 3D high temperature air-flow field's refractive index $f(x,y)$ is

$$\bar{f}(x,y) = \sum_{i=0}^{M-1} \sum_{j=0}^{N-1} \bar{f}(id_x, jd_y) \times rect\left[\frac{1}{d_x}(x - id_x)\right] rect\left[\frac{1}{d_y}(y - jd_y)\right], \tag{17}$$

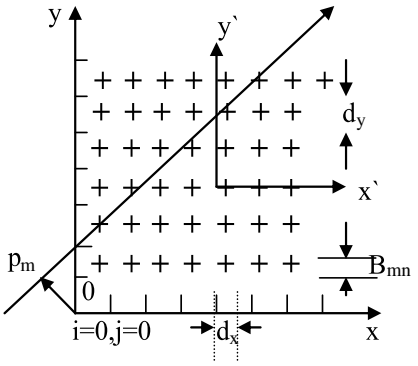

Fig. 4. Rectangular function image of Refractive index $f(x, y)$.

where $\bar{f}(id_x, jd_y)$ can be obtained from formula (15), and the coefficient W_{ij} can be obtained by formula (18):

$$W_{ij}(p_m, \xi_n) = \begin{cases} (1+\tan^2\xi_n)^{1/2} d_x \\ \cdots |B'_{mn}| \le (d_y - d_x|\tan\xi_n|)/2 \\ \cdots \quad \text{and} \quad |\tan\xi_n| > d_y/d_x \\ [(1+\tan^2\xi_n)^{1/2} d_y/|\tan\xi_n| \\ \cdots |B'_{mn}| \le (d_x|\tan\xi_n| - d_y)/2 \\ \cdots \quad \text{and} \quad |\tan\xi_n| > d_y/d_x \\ [1+\tan^2\xi_n)^{1/2}/|\tan\xi_n|][(d_x|\tan\xi_n| + d_y)/2|B'_{mn}|] \\ \cdots \left| \dfrac{d_y - d_x|\tan\xi_n|}{2} \right| < |B'_{mn}| \le \dfrac{d_y + d_x|\tan\xi_n|}{2} \\ d_y \cdots |C'_n| < \dfrac{d_x}{2} \quad \text{and} \quad |\tan\xi_n| = \infty \\ 0 \cdots |B'_{mn}| > (d_x|\tan\xi_n| + d_y)/2 \end{cases} \tag{18}$$

where $C'_n = p_n + id_y$. B'_{mn} is given in formula (14).

According to different observation angle θ and different radial value y', the deflection angle value of light beam can be obtained:

$$A = K_1 \times K_2, \tag{19}$$

where K_1 is the observation data of different directions; K_2 is the observation direction data according to different radial value. These data will make up a linear equational group of unknown f_{ij}

$$B = W_{ij} f, \tag{20}$$

where B is the deflection angle data vector of A; f is the unknown refractive index data vectors of $L = M \times N$, W_{ij} is a matrix consisting of $A \times L$ coefficients. Adopting iterative rebuild arithmetic, we can obtain

$$f^{(0)} = W^z B, \quad \text{and} \tag{21}$$

$$\begin{cases} f^{(p)} \\ \left(\sum_n^{MN} W_{mn} = 0 \right) \\ f^{(p)} + \lambda^{(p)} \dfrac{\omega_{mp} - \sum_n W_{mn} f_n^{(p)}}{\left(\sum_n^{MN} W_{mn} \right)^2} W_{mp}, \\ \left(\sum_n^{MN} W_{mn} \neq 0 \right) \end{cases} \tag{22}$$

where p is the iterative time; W^Z is the transposed matrix; W_{mp} is the vector making up the m_p line elements of matrix W_{ij}; ω_{mp} is the deflection angle of corresponding light line; $\lambda^{(p)}$ is the relaxation parameter.

For higher temperature air-flow field, the calculation method of refractive index difference is:

$$f(x, y) = [1 - T_0/T_D(x, y)](n_0 - 1), \tag{23}$$

where T_0 is the air temperature in room, and $T_D(x, y)$ is the temperature of simulated temperature field. After obtaining the refractive index difference distribution of simulated temperature field, the deflective angle of light line $\omega(y', \xi)$ can be obtained.

4. The Design of Multi-direction Moire Deflection System

For the dissymmetrical temperature air-flow field, multi-direction coinstantaneous note interference pattern needs to be analyzed in order to obtain the 3D space distribution of temperature field refractive index. D. W. Sweeney and C. M. West[3] have utilized the multi-direction holographic interferometry to measure dissymmetrical natural convection pinnate flow 3D temperature field distribution; Maruyama *et al.* used Mach–Zehnder interferometer to obtain the multi-direction deflection pattern of tested 3D temperature field by means of rotating the tested 3D field in turn. However, the method above could not reflect the natural situation of tested 3D temperature field truly. In this paper, CCD grating is adopted as the main component to design a simple optical path to cause large-caliber 3D temperature field multi-directions MOIRE chromatography deflection system. This is shown in Fig. 5.

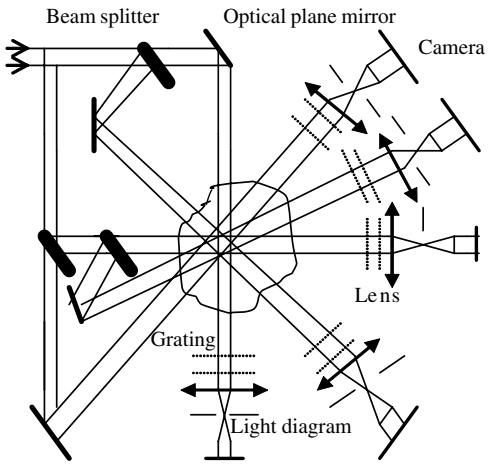

Fig. 5. Multi-direction Moire deflection system.

There are five detective light paths to be designed. Each detective light path has parallel-placed the same period grating G. Adjust the space and angle of the two gratings, the Moire horizontal reference stripes would be clearer and the stripe space would be suitable. The filtering hole on the lens' focal plane can avoid unorderly high-frequency part interfering with Moire pattern.

5. Experiment and Discussion

5.1. *Utilize the multi-direction Moire deflection system to do a simulation test of dual-core flame*

In the experiments, the simulative dissymmetrical temperature field Moire deflection pattern was obtained from five different directions. The obtained projection data are suitable for the complete data rebuilding. According to the multi-direction Moire deflection system, the dual-core flame temperature distribution is mapped by means of using the computer simulation arithmetic.

5.2. *The stability requirement of experimental device*

Moire chromatography technique takes the deflection angles of light beams as the projection data, but the measurement of deflection angle is not like the measurement of optical path difference in interferometry, which needs the reference beam, and the stability requirement of experimental device is not so harsh, so it is convenient for test in locale.

5.3. *The observation angle of multi-direction Moire deflection system*

The observation angle of Multi-direction Moire deflection system is wide; it can record the multi-direction interference pattern in the range of 180°. In the interference pattern, the interference stripes appear sharp, with high resolution. Because each light path is separate, the performance is good.

5.4. *The characteristic of multi-direction interference system*

When most multi-directional interference systems reappraise the temperature field distribution based on the multi-directional interference patterns obtained, they all suppose that the light is beeline through the tested temperature field. In fact, the medium density can cause the light to be deflected. The deflection cannot be ignored. When we analyze the interference pattern, the imaging lens action of observation stripes pattern or screen stripes pattern must be taken into account and adjusted by means of the imaging lens. Moreover, multi-direction Moire deflection system measures the refractive index of tested field by means of deflection effect of tested field when the light is through the tested field, so this method avoids the error caused by light deflection.

6. Application Prospect of Multi-direction Moire Chromatography Optical System

6.1. *The application in aerodynamics and fluid visual observation measurement*

The multi-direction Moire chromatography technique can be used to study the aerodynamics, fluid visual observation, plasma diagnostics, heat conduction and measurement of material transfer etc. If the object is in the form of force, the light path will change, then according to that, the change of transparent object can be analyzed by means of this system.

6.2. *Application of Moire technique to monitor dam deformation*

Computerized tomography (CT) technique is a kind of technique which can rebuild the 2D image of

object's specific levels and form the 3D image according to the 2D image built. In recent years, the technique has been applied in the fields of industry, earth physics, and dam monitoring. In Italy and Japan, it is applied in the diagnosis of dam; the security checks and engineering treatment of dam have good results. Because the CT technique can elicit the 3D image, which can reflect the material's distribution and location of bug truly, we can apply it to control the dam geological structure, find out the distribution of faultage broken area, and the range and extent of rock relaxation before digging the tunnel. CT technique exerts important action in the location, construction and operation period of dam. It not only reduces the complexity of device, but also improves the security of dam. This technique can have significant applications for the internal behavior detection, defect search and aging evaluation.

6.3. *Application in medical engineering*

The application prospect of Moire chromatography optical system which combines computerized tomography technique will have wide application in medicine.[5] It can improve the chest tumor diagnosis, and help to recognize the etiology and pathogenesis for diagnosis and prevention measures.

References

1. Tabea, K., Shirai, H. *et al.*, "Temperature and/or density measurements of asymmetrical flow fields by means of the Moire–Schlieren method[J]," *JSME Int. J., Ser. II* **33**(2), 249 (1990).
2. Dapeng, Y., Zhaoqing, Z. and Anzhi, H., "Al-time tomography of three-dimensional temperature field," *SPIE* (1993).
3. Sweeney, D. W. and Vest, C. M., "Measurement of three-dimensional temperature fields above heated surfaces by holographic interferometry," *Int. J. Heat Mass Transfer.* **17**, 1443–1454 (1974).
4. Kang, Q., Gao, Y., Ding, H. *et al.*, "Study on 3-D arc plasma fields with holographic interferometry," *Chin. J. Lasers (E.E.)* **1**(3) 269–276 (1992).
5. Faris, G. W. and Byer, R. L., "Three-dimensional beam deflection optical tomography of a supersonic jet," *Appl. Opt.* **27**(24), 5200–5212 (1988).